JOURNAL OF EXPERIMENTAL ZOOLOGY 289:385–403 (2001)

Assessing Morphological Differences in an Adaptive Trait: A Landmark-Based Morphometric Approach

R. CRAIG ALBERTSON[1*] AND THOMAS D. KOCHER[1,2]
[1]*Department of Zoology, University of New Hampshire, Durham, New Hampshire 03824*
[2]*Program in Genetics, University of New Hampshire, Durham, New Hampshire 03824*

ABSTRACT East African cichlid fishes have evolved a stunning array of oral jaw morphologies. To better understand the adaptive evolution of this trait, we performed a morphological analysis of the jaws of two closely related species from Lake Malawi that have very different modes of feeding. *Labeotropheus fuelleborni* forages along the substrate with a "biting" mode of feeding, while *Metriaclima zebra* feeds in the water column with a "sucking" mode. We analyzed each of the four skeletal elements that make up the oral jaws: the dentary, articular, premaxilla, and maxilla. In addition, we performed the same analysis on the neurocranium, an element closely associated with the oral jaws. We used the thin-plate spline method to quantify morphological differences, which allowed us to relate our results to the functional biology of the species. We find many aspects of shape change that relate directly to the functional design of the cichlid head. The same series of measurements was made on hybrids between *Labeotropheus* and *Metriaclima*. For every character, hybrid progeny are statistically different from both parental species. These results suggest an additive mode of action of the alleles responsible for these phenotypes. *J. Exp. Zool. 289:385–403, 2001.*

The cichlid fishes of East Africa are a spectacular example of evolutionary radiation. Each of the three large lakes in the region (Victoria, Tanganyika, and Malawi) contains a "flock" of several hundred cichlid species (Fryer and Iles, '72; Echelle and Kornfield, '84). Molecular and geological studies suggest that these radiations are extremely recent (Greenwood, '74; Owen et al., '90; Meyer, '93; Kocher et al., '95; Seehausen, '97). For instance, Lake Malawi is less than 1 MY old (Meyer et al., '90), but contains a flock of well over 500 species (Ribbink et al., '83), and much of this radiation probably occurred within the past several thousand years (Owen et al., '90).

The morphological diversification among Lake Malawi cichlids is of a magnitude normally found only among families of teleosts (Greenwood, '74). Key to their success has been the diversification of the oral jaw apparatus, which has allowed them to evolve many different specialized modes of feeding.

In this study we assess shape differences of the individual skeletal elements of the oral jaws in two rock-dwelling cichlids from Lake Malawi, *Labeotropheus fuelleborni* and *Metriaclima zebra*, and their F_1 hybrid progeny. We employ geometric morphometrics, which gives us tremendous power to discriminate overall shape differences between these three groups. Moreover, a geometric approach maintains a closer relationship to true biological form than do simple linear measurements between landmarks.

FUNCTIONAL MORPHOLOGY AND ADAPTIVE RADIATION

There is a large body of literature devoted to interpreting the functional morphology of the cichlid feeding apparatus. Three major modes of feeding have been identified: sucking, biting, and ram feeding. These three modes are easily predicted from the functional design of the cichlid head (Liem, '91). For instance, the most efficient design for suction feeding is a cone-shaped buccal cavity and a highly protrusible upper jaw that allows for rapid expansion of the buccal volume. On the other hand, streamlined predators have a more cylindrical buccal cavity that cannot produce much suction, but are optimized for the pursuit and overtaking of prey, also known as ram feed-

Grant sponsor: NSF; Grant number: IBN 9905127.
*Correspondence to: R. Craig Albertson, Department of Zoology, University of New Hampshire, 46 College Road, Durham, NH 03824. E-mail: craiga@hopper.unh.edu
Received 8 August 2000; Accepted 5 January 2001

ing (Liem, '91). Biting fish require shifts in anatomical points on the premaxilla, maxilla, and mandible to increase the biting force (Otten, '83).

Most cichlids employ more than one strategy of prey capture, and they possess skulls of intermediate design that will allow them to feed on a variety of foods. For example, *M. zebra* has been characterized as a "biter" (Witte, '84), but will often employ a "sucking" mode when feeding on plankton in the water column (McKaye and Marsh, '83; Ribbink et al., '83; Reinthal, '90). Rather than viewing individual species as specialists, we should consider the balance each has struck among conflicting structural demands (Liem, '80; Barel, '83).

GEOMETRIC MORPHOMETRICS

A geometric approach to shape analysis is based on landmark data (i.e., anatomical points inferred to be homologous between specimens). Landmark positions are recorded in terms of a Cartesian coordinate system, such that each point's (x, y) position can be plotted on a graph.

Geometric morphometrics offer several advantages over traditional morphometrics. First, a landmark-based approach emphasizes the geometry of a given structure, allowing shape change to be reported relative to other structures. Moreover, geometric morphometric results are basis-invariant. That is, results do not depend on arbitrary choices, such as the selection of shape variables or the baseline to be used. Finally, results can be reported via pictorial representations of the structure/organism, rather than just tables of numerical coefficients (Rohlf and Marcus, '93).

Our approach to shape analysis of the cichlid head is unique in several ways. We focus on individual skeletal elements, which allows us to examine aspects of morphology that might otherwise be hidden or confounded when viewing the articulated skeleton or external morphology. We also employ a geometric approach rather than traditional methods of shape analysis, which provides a more precise biological representation of shape differences. The union of these two approaches should offer a more comprehensive understanding of the differences in oral jaw morphology among species.

MATERIALS AND METHODS

Animals and husbandry

Lake Malawi rock-dwelling cichlids (mbuna) are classified into 13 genera that differ primarily in trophic morphology (Moran et al., '94). *M. zebra* and *L. fuelleborni* (Fig. 1), referred to as MZ and LF from here on, are two mbuna species that have evolved very different oral jaw morphologies.

MZ is characterized by a moderately sloped head, a terminal isognathus mouth, and a swollen, horizontally directed vomer (Stauffer et al., '97). When feeding, MZ typically combs loose diatoms from filamentous algae beds while oriented perpendicular to the substrate. This species will also leave its territory in order to feed on plankton in the water column, where it uses a suction mode of feeding (McKaye and Marsh, '83; Ribbink et al., '83; Reinthal, '90).

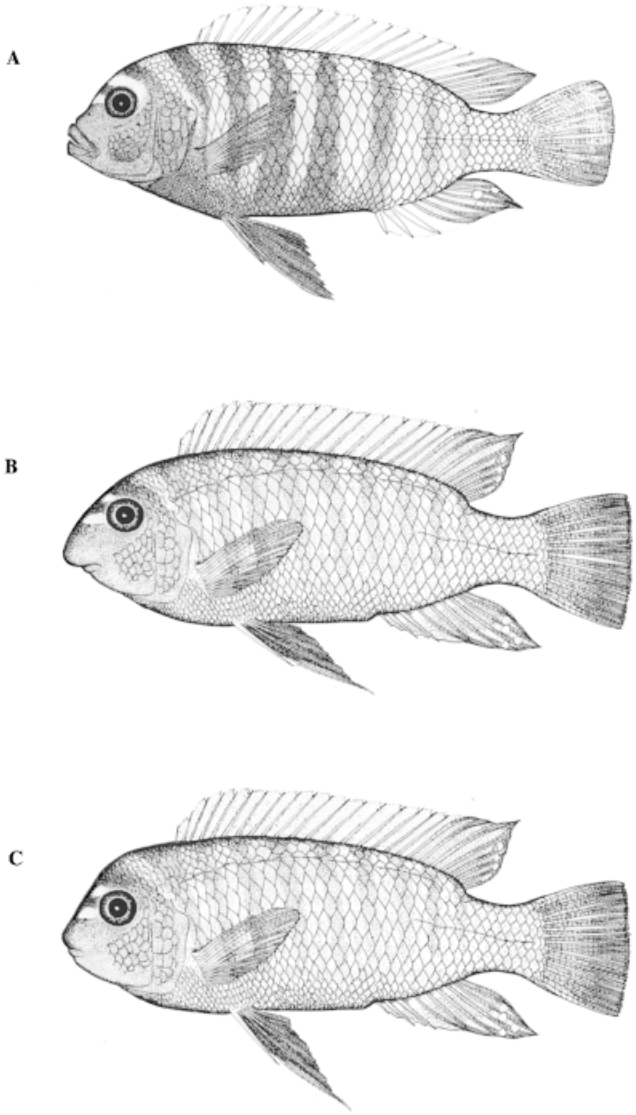

Fig. 1. Specimens used in morphometric study. **A**. *M. zebra* **B**. *L. fuelleborni* **C**. F_1 hybrid.

LF has a large fleshy snout and an inferior-subterminal mouth that it uses to crop algae from rocks while oriented nearly parallel to the substrate (Ribbink et al., '83). Gut analysis and direct observation reveal that the primary diet of LF is attached algae, removed from the rock surface using a biting mode of feeding (Ribbink et al., '83; Reinthal, '90). The orientation of its mouth allows LF to forage in shallow water where surge is a prominent part of the environment, and heterospecific competition is reduced (Ribbink et al., '83).

Parental specimens used in this study were laboratory-reared F_1 animals generated from wild-caught stock. Hybridization, which has been observed to occur among cichlids under no-choice conditions (Loiselle, '71; Crapon de Caprona and Fritzsch, '84; McElroy and Kornfield, '93; personal observation), was achieved by crossing male LF with female MZ in 500-gallon pools containing one male for every four or five females.

All mbuna species are mouth-brooders. Brooding females were transferred to 10-gallon tanks to incubate their clutch. Incubation in the laboratory averaged about three weeks for both species. Females were removed from the tank after they released their young. Fry were reared in 10-gallon tanks for approximately three months. They were then transferred to 50-gallon tanks for an additional two to three months. Finally, families were moved to 500-gallon pools where they were allowed to grow to sexual maturity (an additional six to eight months). Because the primary diet of these species in the wild is algae (Reinthal, '90), all specimens were reared on high-quality spirulina flake food (Aquatic Ecosystems, FL). A diet of flake food was chosen to minimize the functional demands on the trophic apparatus.

Preparation of specimens

Animals were collected no earlier than 12 months of age, and more typically at 18 months. Fifty specimens were used in this study, 15 of each parental species and 20 F_1 hybrids. Animals were sacrificed with MS222 in accord with a protocol approved by the University of New Hampshire ACUC. Specimens were then prepared for morphometric analysis using dermestid beetles, which cleaned and disarticulated skeletal elements of the head. Afterward, elements were bleached with 10% H_2O_2.

Images of individual elements were captured using a SPOT digital camera (Diagnostic Instruments, Inc.) mounted on a Zeiss SV11 dissecting scope. Images were imported into NIH Image (version 2.1), and landmark positions were scored as (x, y) coordinates. Descriptions of landmarks are found in Table 1.

Superimposition of landmark data

Superimposition of landmark data was performed using a Procrustes generalized least-squares fit (GLSF) algorithm (Gower, '75; Rohlf and Slice, '90) in Morphometrika 7.0 (Walker, '99). A least-squares approach will superimpose configurations so that the sum of squared distances between corresponding landmarks is minimized. This is achieved by scaling, translating, and rotating specimens with respect to a mean consensus configuration. A potential disadvantage to this approach arises when the difference between forms is localized to one or few landmarks. In this situation, GLSF may distribute localized variance over multiple landmarks, making the way variance is allocated to individual landmarks an artifact of the method. Procrustes generalized resistant-fit (GRF) superimposition compensates for this problem by using a more complex, and computationally expensive, approach of regression using repeated medians (Rohlf and Slice, '90). Because LF and MZ differ dramatically over the entire structure for most elements, we used GLSF rather than the GRF algorithm. The only possible exception to this trend is found in the neurocranium, where LF and MZ differ most dramatically in the anterior region of the skull. We performed both GLSF and GRF superimposition for this structure and found no difference in the results (not shown).

Thin-plate spline analysis

Thin-plate spline (TPS) analysis was performed in Morphometrika 7.0 (Walker, '99). The TPS technique rigorously implements D'Arcy Thompson's concept of Cartesian grid deformations (Thompson, '17). A thorough description of the technique may be found in Bookstein ('89, '91). In short, TPS models the form of an infinitely thin metal plate that is constrained at some combination of points but is otherwise free to adopt the target form in a way that minimizes bending energy. In morphometrics, this interpolation is applied to a Cartesian coordinate system where deformation grids are constructed from two landmark configurations (Bookstein, '91).

Thin-plate spline analysis is valuable for several reasons. First, the TPS technique is independent of any anatomical frame of reference. That is, the position of each landmark is evaluated rela-

TABLE 1.

Element	Landmarks	Descriptions (after Barel et al., '76)
Lower jaw (lateral)	1	Rostral tip of the dentary
	2	Tip of the rostral process of the articular
	3	Dorsal tip of the coronoid (dentray process)
	4	Dorsal tip of the primorial (articular) process
	5	Dorsal process of the suspensoriad articulation facet
	6	Postarticulation process (of the suspensoriad articulation facet)
	7	Retroarticular process
	8	Rostral process of the coulter area
Lower jaw (ventral)	1	Lateral-most point of the dentigerous area
	2	Oral-most point of the symphyseal facet
	3	Rostral process of the coulter area
	4	Postarticulation process (of the suspensoriad articulation facet)
	5	Lateral-most point of suspensoriad articulation facet
Maxilla	1	Medial process of the premaxillad wing
	2	Medial process of the palatinad wing
	3	Lateral process of the palatinad wing
	4	Shank process
Premaxilla	1	Rostral-most point of the dentigerous arm
	2	Dorsal process of the ascending spine
	3	Ventral-most point of the interprocess edge
	4	Dorsal process of the maxillad spine
	5	Caudal process of the dentigerous arm
Neurocranium	1	Rostral tip of the vomer
	2	Caudal-most point of the preorbital ridge
	3	Tip of preorbital process
	4	Dorsal tip of the supraoccipital crest
	5	Ventral process of the vertebrad concavity
	6	Pharyngobrachiad apophysis
	7	Tip of postorbital process
	8	Caudal-most point of the vomerine-palatinad articulation facet
Vomer	1	Rostral tip of the vomer
	2	Rostral edge of the vomerine notch
	3	Rostral edge of the vomerine-palatinad articulation facet
	4	Doral crest of the parashenoid, on the line connecting the preorbital processes

tive to all other landmarks rather than to a single point. This method also allows for the objective generation of deformation grids. Finally, the total deformation of the thin-plate spline can be decomposed into geometrically orthogonal components based on scale (Rohlf and Marcus, '93; Yaroch, '96). These components (partial warps) can be localized to describe precisely what aspects of shape are different. Partial warp scores are also the shape variables used in multivariate analyses.

Multivariate analysis of TPS data

For each skeletal element a discriminant function analysis was performed using SPSS (version 6.0 for Macintosh) on all shape variables (partial warp scores, including the uniform component). Results from this test were used to assess group differences for each skeletal element, and to estimate the magnitude of shape difference between the parental species. Since the first Canonical Variate axis best represents interspecific shape differences, results are only presented for CV1.

To estimate the relative contribution of each shape variable in the discriminant function analysis, a multivariate regression was performed for each skeletal element using TPSregr (Rohlf, '99). Regression analysis was used to assess the relationship between shape variables and scores on the Canonical Variate axis. In terms of partial warps, the model follows:

$$\text{Shape}(\text{PW1}x, \text{PW1}y, \text{PW2}x, \text{PW2}y, \ldots, \text{PW0}x, \text{PW0}y) = \text{Constant} + (m)\text{CV1 score}$$

Furthermore, TPSregr allows for the deformation of shape, as interpreted by each canonical variate axis, to be visualized as a deformation grid or associated vector displacements, allowing for a more exacting biological interpretation of the discriminant function analysis.

RESULTS

A multivariate analysis of variance (MANOVA) showed that mean differences among LF, MZ, and F_1 along CV axes were unlikely due to chance, Wilk's $\Lambda = 0.00433$, $F(12, 72) = 85.2$, $P < 0.0001$. Likewise, univariate F-tests for each element revealed significant mean differences among groups ($P < 0.0001$ in every case).

Disarticulated skeletal elements are shown in Figs. 2–7. Below, results are described both qualitatively as landmark variation after superimposition and quantitatively as deformations after the multivariate analysis of shape variables (Figs. 9–14). Table 2 lists (1) the variation explained by the first canonical variate axis; (2) the number of standard deviation units which separate the parental species along CV1; and (3) the relationships between shape variables and CV1.

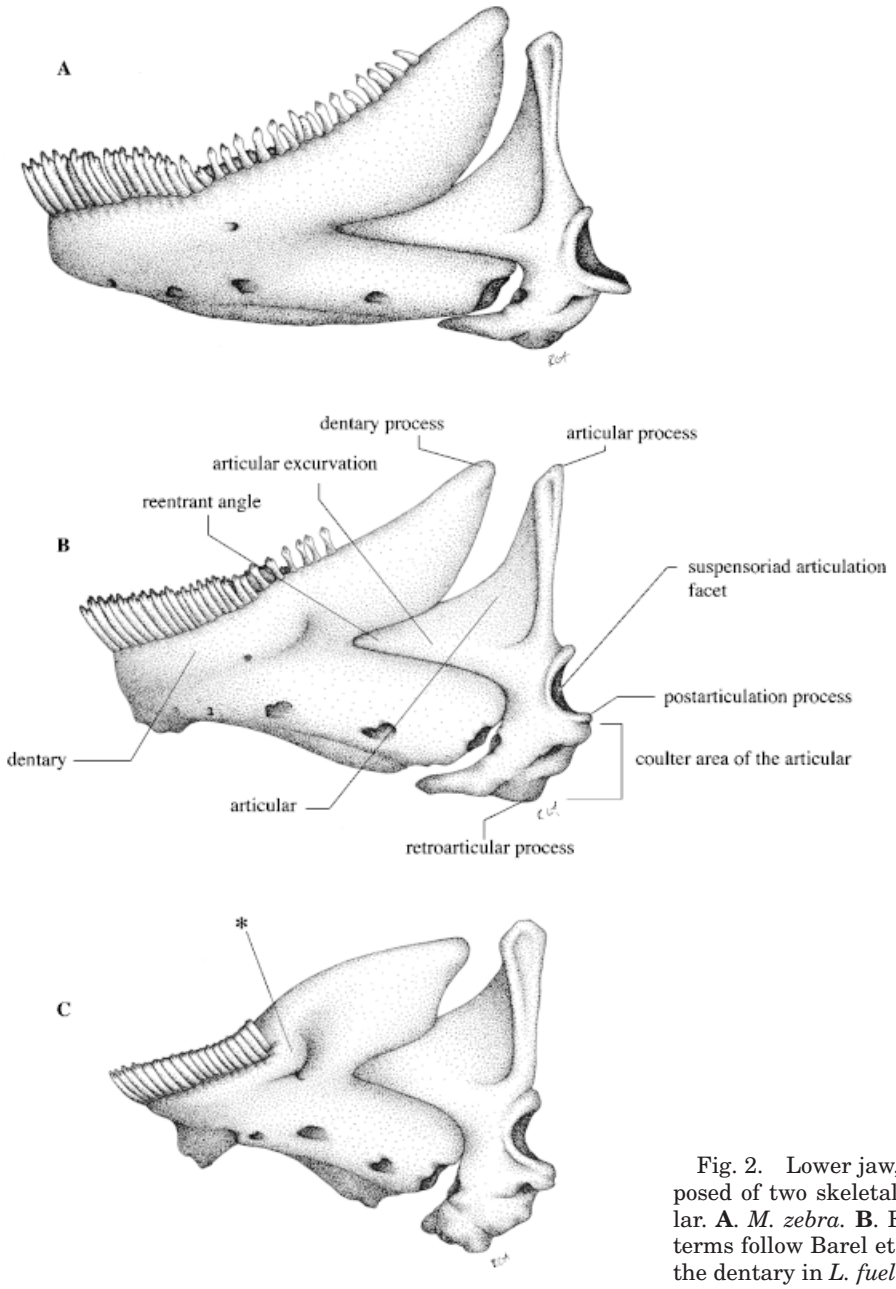

Fig. 2. Lower jaw, left lateral view. The lower jaw is composed of two skeletal elements: the dentary and the articular. **A**. *M. zebra*. **B**. F_1 hybrid. **C**. *L. fuelleborni*. Anatomical terms follow Barel et al. ('76). *Note the lateral expansion of the dentary in *L. fuelleborni*.

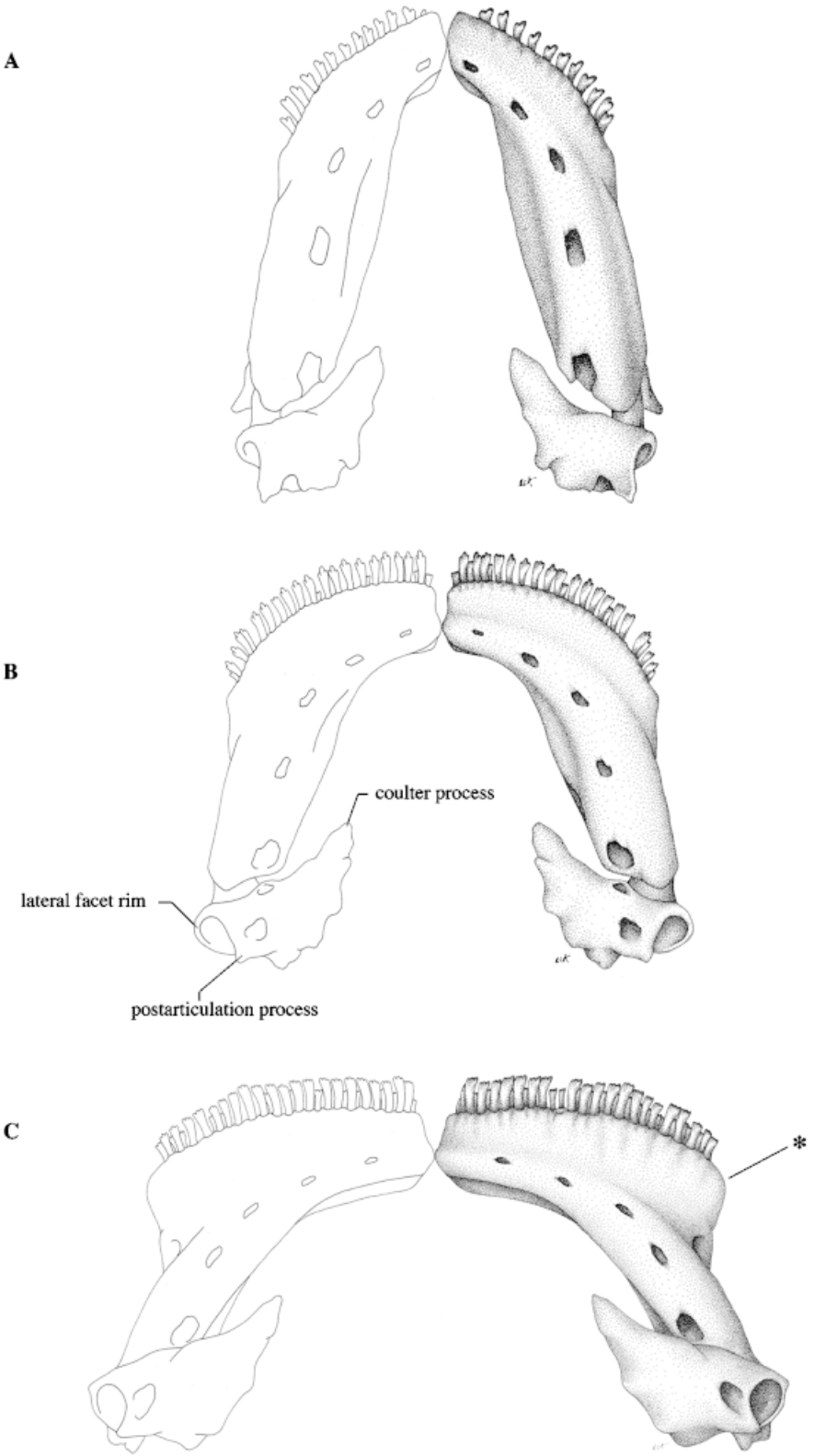

Fig. 3. Right and left halves of the lower jaw in the ventral view. **A**. *M. zebra*. **B**. F_1 hybrid. **C**. *L. fuelleborni*. Anatomical terms follow Barel et al. ('76). *Note the lateral expansion of the dentary in *L. fuelleborni*.

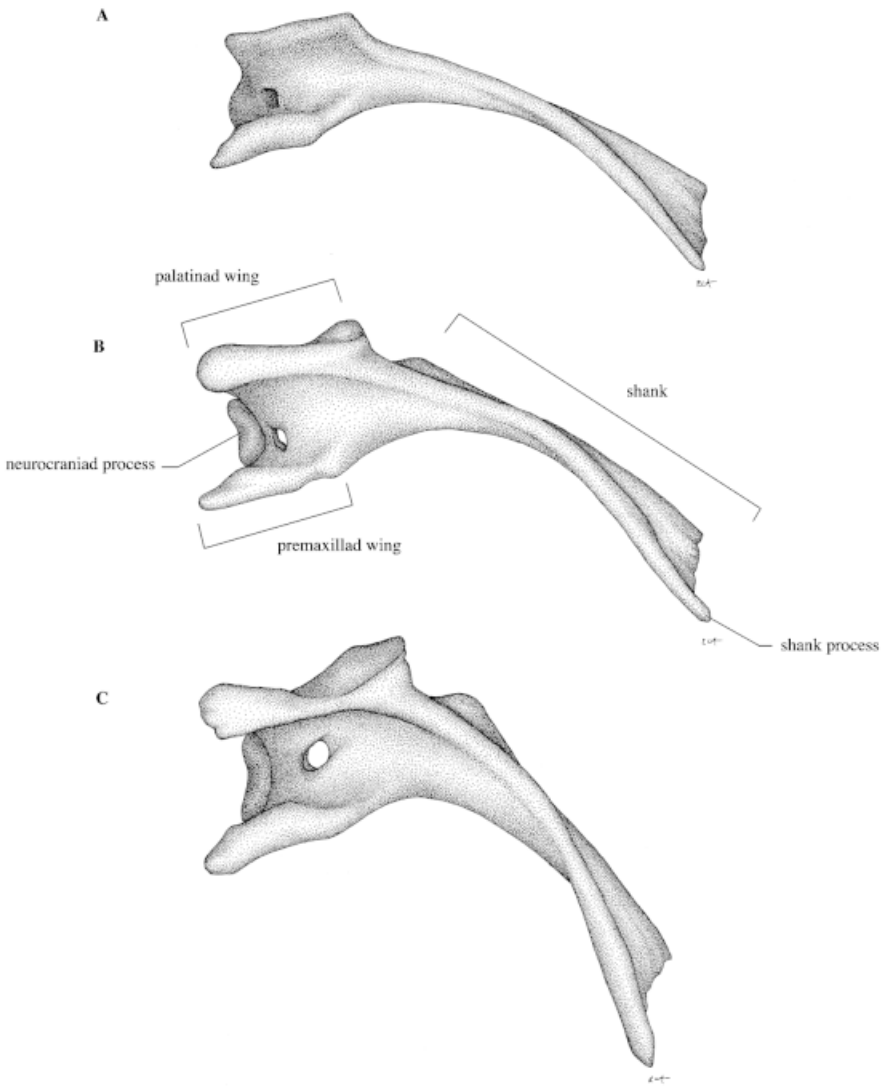

Fig. 4. Maxilla in the right rostral view. **A**. *M. zebra*. **B**. F_1 hybrid. **C**. *L. fuelleborni*. Anatomical terms follow Barel et al. ('76).

Lower jaw (lateral view)

After GLSF superimposition (Fig. 8b), landmark variation around the consensus configuration is distributed over most landmarks in the lateral view of the lower jaw. However, variation around landmarks one and four describes most interspecific difference.

The lower jaw in teleosts is composed of two ontogenetically distinct elements. The anterior portion that bears the teeth is the dentary, while the more posterior region that articulates with the suspensorium is the articular. These two bones are both developmentally and functionally discrete. Differences revealed by the first canonical variate axis (Fig. 8c,d) deal with relative shape differences between these two elements. In MZ, the height of the articular is reduced relative to the length of the dentary, which is dramatically elongated. There is also a pronounced and localized lengthening of the ventral process of the suspensoriad articulation facet relative to the rest of the articular. On the other hand, LF is characterized by a dramatic increase in the height of the articular relative to a pronounced shortening of the dentary.

Lower jaw (ventral view)

Landmark variation is distributed over landmarks one, two, and five in the ventral view of the lower jaw (Fig. 9b). Variation around land-

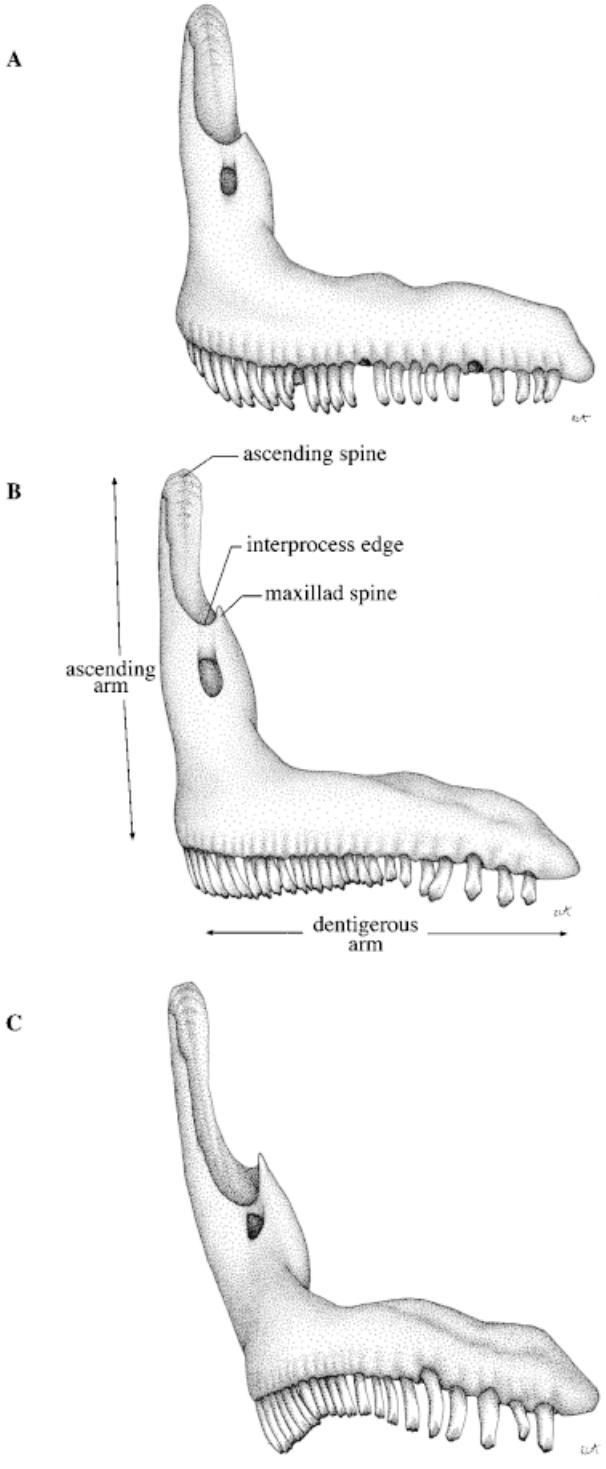

Fig. 5. Premaxilla in the left lateral view. **A**. *M. zebra.* **B**. F_1 hybrid. **C**. *L. fuelleborni*. Anatomical terms follow Barel et al. ('76).

marks one and two, which represent the mandibular symphysis and the lateral-most point of the dentary, captures variation in the width of the dentary. Along the anterio-posterior axis, most variation is observed at landmark five, which is the rostral tip of the coulter process.

The first canonical variate axis characterizes equivalent aspects of interspecific shape change (Fig. 9c,d). The major aspect of shape change deals with the width of the lower jaw. There is a dramatic increase in the width of the lower jaw in LF relative to MZ. However, more subtle aspects of shape difference are revealed by the analysis. For example, the most extreme difference in jaw width is localized to the dentary, with difference in the width of the articular being less pronounced. In LF, an increase in the width of the dentary is accompanied by a relative lengthening of the coulter region of the articular. There is also a pronounced and localized shortening of the ventral process of the suspensoriad articulation facet in LF. In MZ, the width of the dentary is reduced, the ventral process of the suspensoriad articulation facet in elongated, and the coulter process is shortened.

Maxilla

After GLSF superimposition (Fig. 10b), landmark variation is distributed in the maxilla over landmarks one, two, and three. Most of this variation is along the medio-lateral axis (the palatine process is taken as lying along the medio-lateral axis). Landmarks two and three lie on opposite ends of this process. Variation in landmark two is slightly skewed toward the anterio-posterior axis. This variation captures not only the length of the palatine process but also the bending of the entire maxilla. Little variation is observed at landmark four.

The first canonical variate axis emphasizes two aspects of shape difference in the maxilla (Fig. 10c,d). The first deals with the length of the palatine process, and the second with the curvature of the entire maxilla. In MZ, there is a shortening of the palatine process relative to the length of the entire element, while in LF the same process is dramatically elongated. In addition, the maxilla is virtually straight in MZ, as opposed to LF where it is distinctly bent.

Premaxilla

Landmark variation around the consensus configuration is distributed over most landmarks in

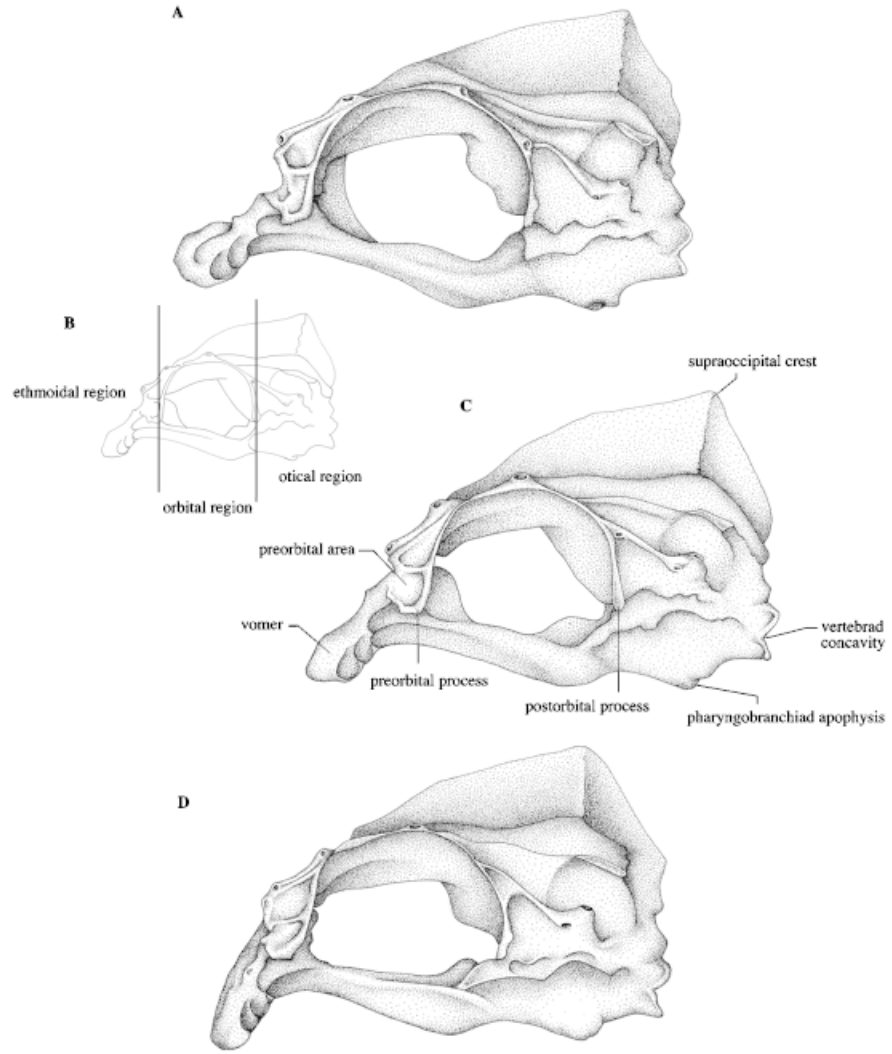

Fig. 6. Neurocranium, left lateral view. **A**. *M. zebra*. **B**. Generalized line drawing, showing three regions of the neurocranium. **C**. F_1 hybrid. **D**. *L. fuelleborni*. Anatomical terms follow Barel et al. ('76).

the premaxilla (Fig. 11b). There is considerable variation around landmarks one and five along the anterio-posterior axis, reflecting the length of the dentigerous arm. Variation around landmark two is largely along the dorso-ventral axis, but it is also slightly skewed toward the anterio-posterior axis. This pattern captures both the length of the ascending arm and the angle formed by the two arms of the premaxilla. There is also variation along the dorso-ventral axis at landmarks three and four associated with the height of the maxillad spine.

The deformation of the premaxilla along CV1 emphasizes several aspects of interspecific shape change (Fig. 11c,d). In MZ, the rostral portion of the ascending arm is elongated relative to the more distal region of the same arm, with localized shortening of both the ascending and maxillad spines. The dentigerous (tooth bearing) arm is also elongated in MZ relative to the ascending arm. In contrast, the rostral portion of the ascending arm is shortened in LF relative to the distal portion, and both the ascending and maxillad spines are elongated. The dentigerous arm in LF is also shortened relative to the ascending arm. Finally, the angle formed by the two arms of the premaxilla is obtuse in LF and acute in MZ.

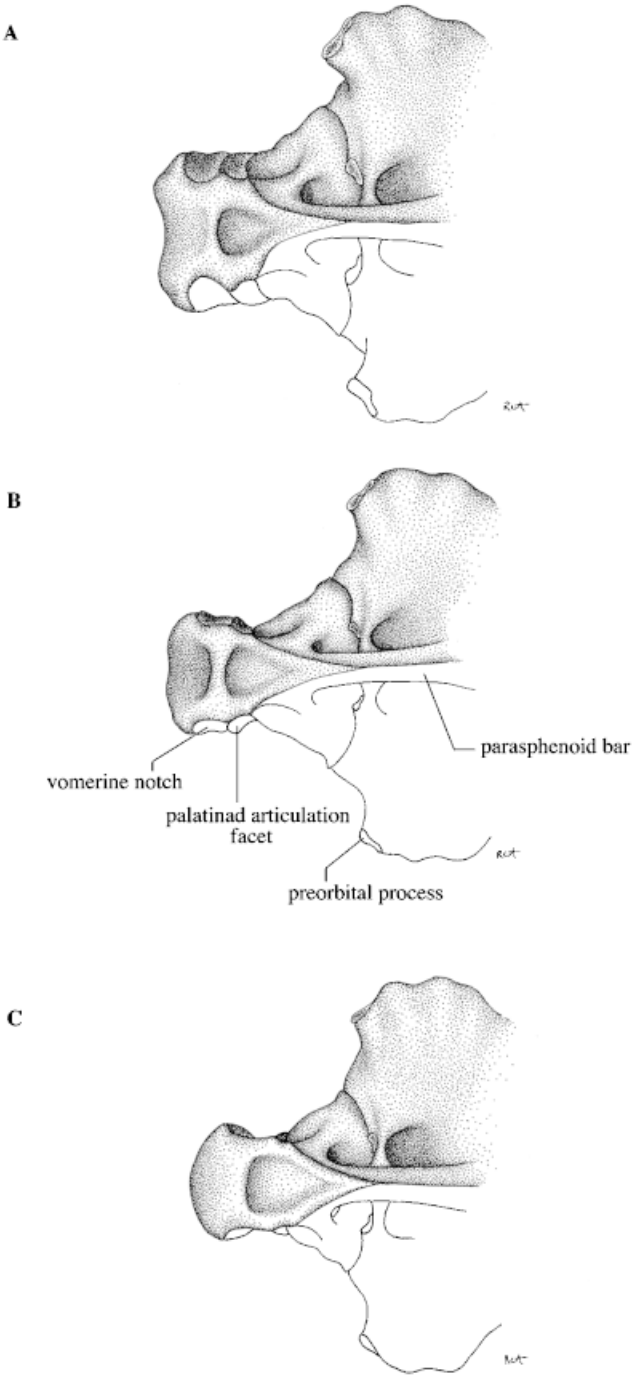

Fig. 7. Ethmoid region of the skull, showing the vomer in the ventral view. **A**. *M. zebra*. **B**. F_1 hybrid. **C**. *L. fuelleborni*. Anatomical terms follow Barel et al. ('76).

TABLE 2.

Element	% variance explained by CU1	#stdev unit between parental species	Significant (P > 0.01) regression coefficients demonstrating the relationship between shape variables and CV1										
			*x*1	*y*1	*x*2	*y*2	*x*3	*y*3	*x*4	*y*4	*x*5	*y*5	*x*0	*y*0
Lower jaw (lateral)	71	13.2	0.4897	0.2363	0.2474	0.3238	0.3534	0.2378	0.7129	0.9523	0.0839	0.8262	0.2603	0.933
Lower jaw (ventral)	90	16.1	0.5746	0.1969	0.9724	N/S							0.8167	0.8827
Maxilla	85	10.3	0.809	0.0785									0.9438	0.8923
Premaxilla	84	11	0.8683	0.5376	0.9352	0.8328							0.4375	0.7584
Neurocranium	55	21.3	0.5923	0.2878	0.1409	0.7167	0.787	0.1696	0.8404	0.5501	0.4834	0.6059	0.8969	N/S
Vomer	58	5.5	0.0812	0.6973									0.7068	0.596

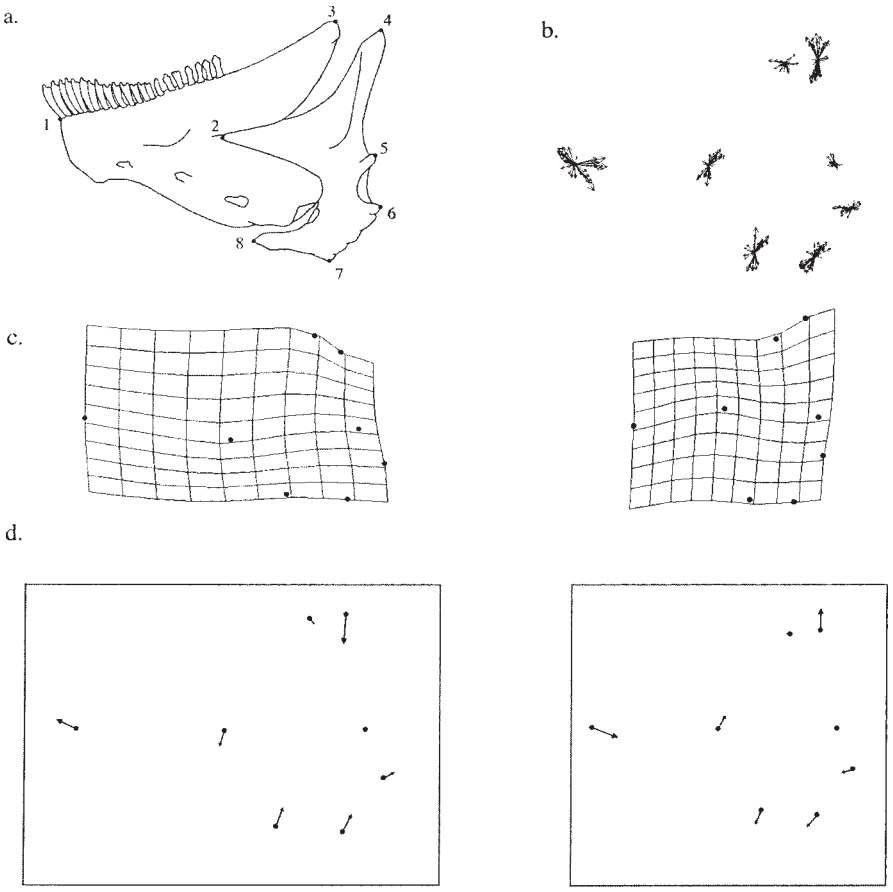

Fig. 8. **a.** Landmark position on the lower jaw in the lateral view. **b.** Landmark variation around the consensus configuration after a generalized least-squares fit superimposition. **c.** Deformation grids as a function of the first canonical variate axis. The figure on the left represents the deformation when the mean form of *M. zebra* is the target. Likewise, the figure on the right represents the deformation when the mean form of *L. fuelleborni* is the target. **d.** Vector displacements which correspond to the deformation grids.

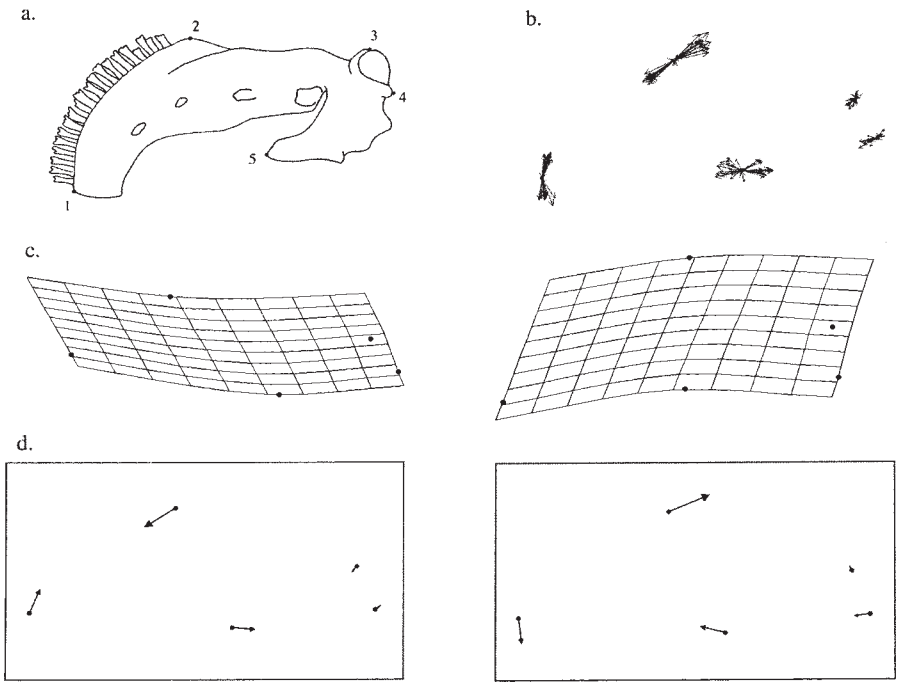

Fig. 9. **a.** Landmark position on the lower jaw in the ventral view. **b.** Landmark variation around the consensus configuration after a generalized least-squares fit superimposition. **c.** Deformation grids as a function of the first canonical variate axis. The figure on the left represents the deformation when the mean form of *M. zebra* is the target. Likewise, the figure on the right represents the deformation when the mean form of *L. fuelleborni* is the target. **d.** Vector displacements which correspond to the deformation grids.

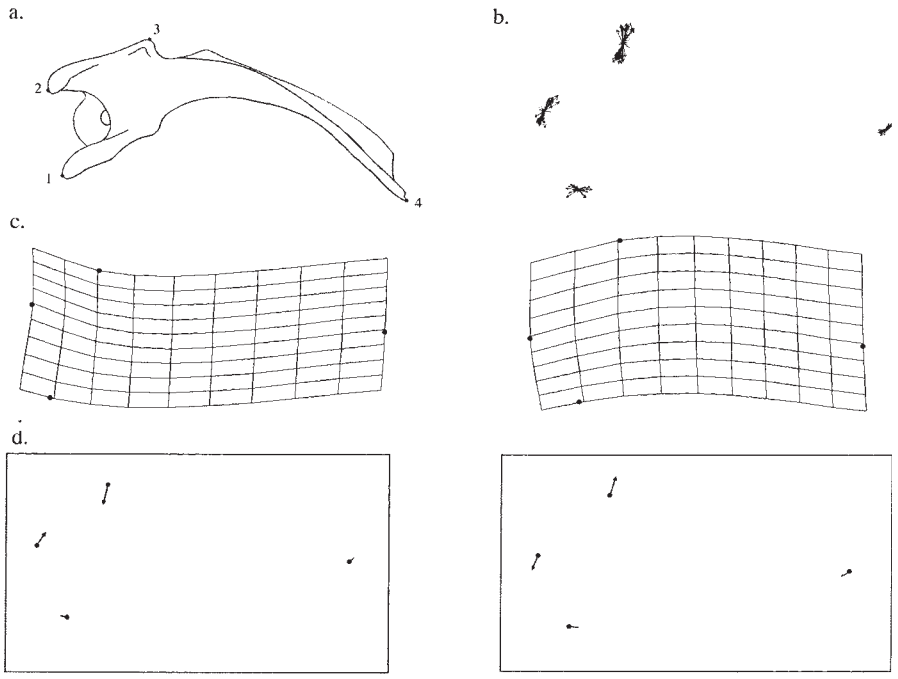

Fig. 10. **a.** Landmark position on the maxilla. **b.** Landmark variation around the consensus configuration after a generalized least-squares fit superimposition. **c.** Deformation grids as a function of the first canonical variate axis. The figure on the left represents the deformation when the mean form of *M. zebra* is the target. Likewise, the figure on the right represents the deformation when the mean form of *L. fuelleborni* is the target. **d.** Vector displacements which correspond to the deformation grids.

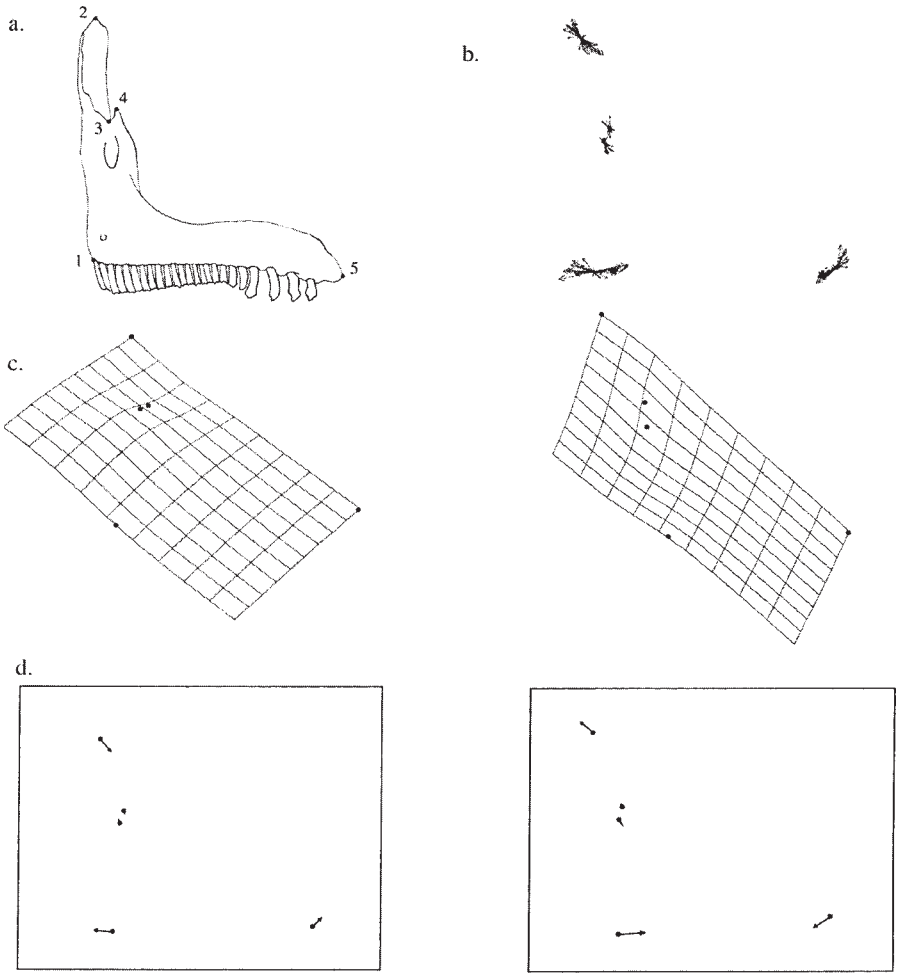

Fig. 11. **a.** Landmark position on the premaxilla. **b.** Landmark variation around the consensus configuration after a generalized least-squares fit superimposition. **c.** Deformation grids as a function of the first canonical variate axis. The figure on the left represents the deformation when the mean form of *M. zebra* is the target. Likewise, the figure on the right represents the deformation when the mean form of *L. fuelleborni* is the target. **d.** Vector displacements which correspond to the deformation grids.

Neurocranium

Landmark variation (Fig. 12b) reveals three aspects of shape variation in the neurocranium. Change in vomer rotation is captured by variation at landmark one. Difference in the length of the preorbital region is identified by variation at landmark two. Finally, variation in the height of the supraoccipital crest is reflected by variation at landmark four.

Deformation of the neurocranium (lateral) along CV1 captures two aspects of interspecific shape change (Fig. 12c,d). The first is vomerine position, and the second is preorbital length. LF has an expanded preorbital area relative to the rest of the skull, while in MZ this area is more attenuated. There is also a horizontal rotation of the vomerine process relative to the rest of the ethmoidal region of the skull in MZ. In LF, the vomerine process is rotated ventrally relative to the ethmoidal region. Deformation as a function of CV1 does not implicate height of the supraoccipital crest as a major source of interspecific shape difference.

Vomer

After GLSF superimposition (Fig. 13b), landmark variation occurs along both the anterio-posterior and medio-lateral axes of the vomer. Variation at landmark two reflects shape change in the width of the vomer, while variation at landmark one identifies change in the length of the vomer. The relative distance between landmarks two and three also varies. This aspect of shape change captures the distance between the vomerine notch (landmark two) and the vomerine palatinad articulation facet (landmark three). There is little variation at landmark four.

The deformation of the vomer as a function of CV1 (Fig. 13c,d) shows that LF and MZ differ in terms of both the width and the roundness of the vomer. The vomer is shown to be wider in MZ than LF. Moreover, in MZ the vomer is expanded (laterally) at the vomerine notch relative to the palatinad articulation facet, while in LF there is no difference in width between these two structures. Thus, interspecific change in the width of the vomer occurs at the vomerine notch, not the palatinad articulation process. Finally, MZ has a blunt vomerine process relative to LF, which has a more rounded vomer.

DISCUSSION

During the early radiation of Lake Malawi's cichlids, an important functional divergence prob-

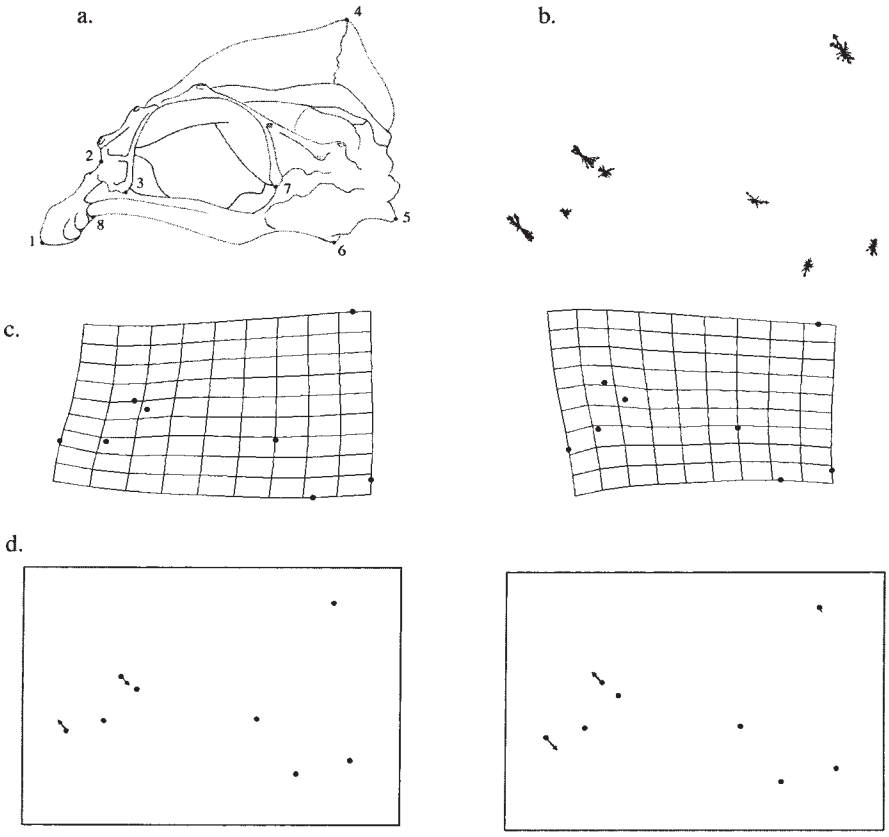

Fig. 12. **a.** Landmark position on the neurocranium. **b.** Landmark variation around the consensus configuration after a generalized least-squares fit superimposition. **c.** Deformation grids as a function of the first canonical variate axis. The figure on the left represents the deformation when the mean form of *M. zebra* is the target. Likewise, the figure on the right represents the deformation when the mean form of *L. fuelleborni* is the target. **d.** Vector displacements which correspond to the deformation grids.

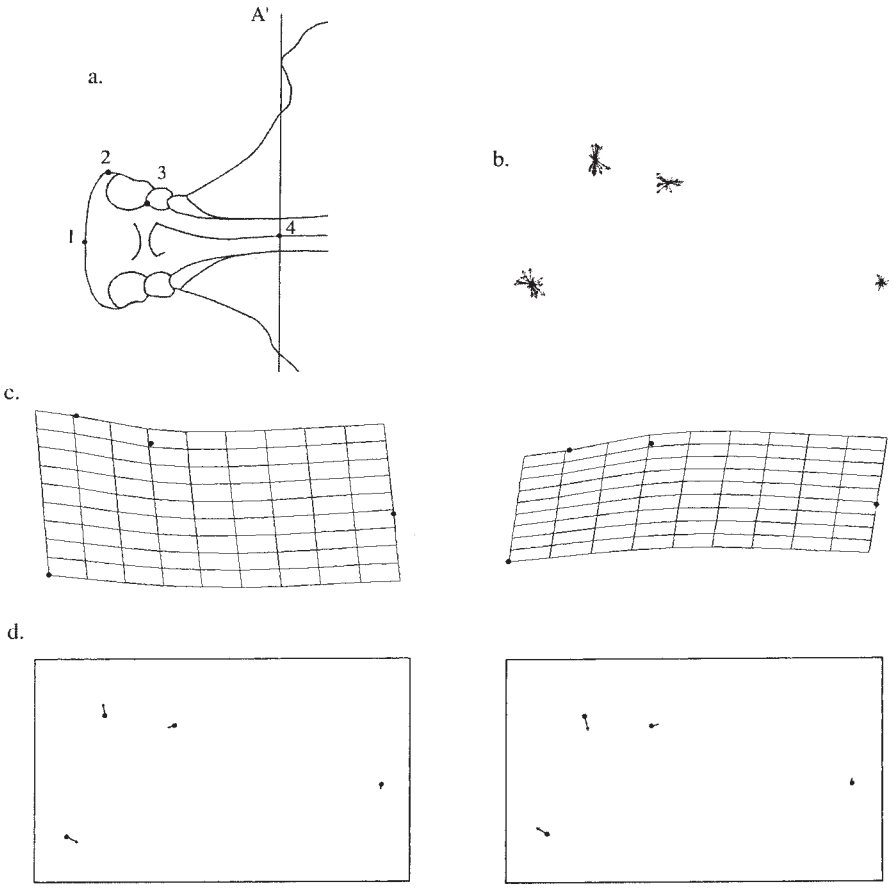

Fig. 13. **a.** Landmark position on the vomer in the ventral view. Here, A′ is the line that connects the preorbital processes. **b.** Landmark variation around the consensus configuration after a generalized least-squares fit superimposition. **c.** Deformation grids as a function of the first canonical variate axis. The figure on the left represents the deformation when the mean form of *M. zebra* is the target. Likewise, the figure on the right represents the deformation when the mean form of *L. fuelleborni* is the target. **d.** Vector displacements which correspond to the deformation grids.

ably occurred between the three basic modes of feeding: biting, sucking, and ram-feeding (Albertson et al., ’99). This same trend has been observed repeatedly in many fishes from post-glacial lakes, including stickleback (*Gasterosteus aculeatus* complex), whitefish (*Coregonus* complex), and arctic charr (*Salvelinus alpinus* complex) (reviewed in Schluter and McPhail, ‘93). We chose MZ and LF because they are closely related species that lie on opposite ends of the biting/sucking continuum. We find many aspects of interspecific shape difference that relate directly to the functional biology of these organisms. Several morphological characters have been identified in the cichlid head that predict feeding performance (Otten, ’83; Liem, ’91). A subset of these, which pertain to MZ and LF, is listed in Table 3 and described in greater detail below.

TABLE 3.

	Lf	Mz
Suction-feeding		
Long ventral process of the suspensoriad articulation facet		X
Attenuated buccal cavity		X
Attenuated neurocranium (Liem, ’90)		X
Abbreviated preorbital region of the skull (Liem, ’90)		X
Enlarged, horizontally directed vomer (Liem, ’90)		X
Biting		
Short ascending arm of the dentary (Otten, ’83)	X	
Wide, robust lower jaw (Liem, ’90)	X	
Curved, robust maxilla (Otten, ’83; Liem, ’90)	X	
Long palatinad wing of the maxilla	X	
Obtuse angle formed between two arms of the premaxilla (Otten, ’83)	X	
Short load-bearing region of the ascending arm of the premaxilla (Otten, ’83)	X	

Form and function

One important difference between MZ and LF involves the ascending process of the articular. This process is where the second adductor mandibulae inserts and is an important lever in the action of jaw adduction (Otten, '83). LF has a substantially higher articular process, suggesting greater force transmission of the adductor mandibulae and therefore a stronger bite. The height of this lever also has major consequences in the speed of jaw rotation. The implication of a shorter articular process in MZ is that this species has a faster jaw closing motion (greater angular rotation).

Both the width and length of the lower jaw differ dramatically between LF and MZ. In LF the jaw is short, wide, and U-shaped. In MZ it is narrow, elongated, and V-shaped. The U-shaped lower jaw of LF is part of a square-shaped buccal cavity, better for taking large bites of algae. In fact, LF has developed pronounced lateral expansions (* in Figs. 3 and 4), just dorsal to the reentrant angle of the articular, which bear teeth and dramatically expand biting surface area. The V-shaped lower jaw of MZ is part of a more attenuated buccal cavity, better for sucking plankton from the water column.

These species also differ in the shape of the suspensoriad articulation facet, which is where the lower jaw articulates with the suspensorium. In MZ the ventral lip of this facet is long, while in LF it is quite short. Because MZ feeds with a sucking action, this long ventral process may be used to support the lower jaw during mouth opening.

The maxilla is more robust in LF than in MZ, presumably because it endures greater force during biting. The first adductor mandibulae inserts into the buccal side of the maxillary shank. This muscle is larger and shifted dorsally in LF (dissection not shown, but it can be accessed on our web site: http://tilapia.unh.edu/morph/morph.html). The maxilla may be more robust in LF to support the action of this larger muscle.

LF also has a much longer and wider palatinad wing of the maxilla. The intermaxillary ligament inserts on the rostral face of this structure. A longer palatinad wing may allow the maxilla to articulate more securely with the premaxilla. Likewise, a larger wing provides greater surface area for the intermaxillary ligament to insert.

The most noticeable difference in the premaxilla involves the relative lengths of the ascending and dentigerous arms. A longer ascending arm in LF facilitates the ventral rotation of the oral jaw (see below). The length of the ascending arm is also correlated with the length of the maxillad spine. This process is much longer in LF than in MZ. The maxillad spine is associated with the maxilla as well as the rostral cartilage. A longer maxillad spine in LF may simply be a consequence of a longer ascending arm. Alternatively, this process may serve to maintain a more effective articulation with both the maxilla and rostral cartilage.

An obtuse angle formed by the ascending and dentigerous arms of the premaxilla allows for greater force transmission during biting (Otten, '83). This angle is obtuse in LF and acute in MZ. Again, LF has a more efficient design for biting.

The premaxilla in LF is an excellent example of how a species evolves under opposing structural and functional demands. How can LF have an inferior-subterminal mouth yet employ a highly specialized biting mode of feeding? A subterminal mouth allows LF to feed while swimming nearly parallel to the substrate. This orientation allows LF to forage in shallow, wave-swept habitats where competition with heterospecifics is minimized. Structurally, this orientation is accomplished by rotating the vomerine process ventrally and elongating the ascending arm of the premaxilla. However, a *shorter* ascending arm of the premaxilla will increase force transmission during biting (Otten, '83). A shorter arm increases biting efficiency, in part, because the distance between the intermaxillary ligament and the rostral tip of the premaxilla is a determinant of biting force: the shorter the distance, the greater the biting force (the intermaxillary ligament lies below the interprocess edge of the premaxilla; landmark 3) (Otten, '83). Although LF has a longer ascending arm than MZ, the distance from the interprocess edge and the rostral tip of the premaxilla (landmarks one and three) is actually shorter in LF than in MZ. The length of the ascending arm in LF is increased by lengthening the ascending spine, not the entire arm. In other words, LF has a long ascending arm to facilitate the ventral rotation of the lower jaw; however, the load-bearing region of this arm is short and robust.

The robust load-bearing area of the ascending arm in LF correlates with an enormous intermaxillary ligament. Species in the genus *Labeotropheus* are characterized by a large fleshy "nose" which wraps around the rostral tip of the upper jaw. This "nose" consists predominantly of the intermaxillary ligament (dissection not shown, but it can be accessed on our web site: http://tilapia.unh.edu/morph/

morph.html). This massive ligament is presumably needed to resist the considerable force applied as the maxillary shank is pulled posteriorly by the adductor mandibulae during biting.

Interspecific shape difference in the neurocranium is limited to two aspects of morphology: vomer position and length of the preorbital region of the skull. MZ, like other species that feed with a sucking mode, has a terminal mouth and a large, horizontally directed vomer. This orientation facilitates jaw protrusion during suction feeding. During suction feeding, the ascending arm of the premaxilla slides along the vomerine process by way of the rostral cartilage, allowing the upper jaw to distend. Upper jaw protrusion serves to increase the volume of the buccal cavity. LF, like other species with a subterminal mouth, has a vertically directed vomer. We also find that MZ has a short, attenuated preorbital region of the skull, while LF has an expanded preorbital region. These shape differences clearly reflect different modes of feeding.

The supraoccipital crest is where the epaxial musculature inserts on the skull. Epaxial muscles are important in head lifting, a critical aspect of suction feeding (Lauder, '79; Liem, '80). Dorso-ventral compression of the supraoccipital crest is thought to occur within cichlid species that maintain close contact with the substrate (Greenwood, '78; Barel, '83). One might expect that the supraoccipital crest would be higher in MZ than in LF. However, we found no difference in this trait between MZ and LF (see Fig. 14). Rather, this element is the source of considerable intraspecific variation. This result is supported by Reinthal ('90) who found that crest height showed a great deal of intraspecific variation among mbuna and was not a good character to distinguish among species.

The neurocranium is a large and functionally dynamic structure; it is associated with the oral jaws via the ethmoidal region of the skull, the pharyngeal jaws by way of the pharyngeal apophysis, and the epaxial musculature via the supraoccipital crest. Interestingly, differences in skull shape between MZ and LF, which have widely disparate jaw morphologies, are limited to the ethmoidal region. That is, shape differences are limited to the region of the skull directly associated with the oral jaw apparatus.

The lateral aspect of the ethmoidal region is much more important in distinguishing MZ and LF than is the ventral aspect of the same region. LF and MZ differ by over 21 standard deviations in the lateral view of the skull, while in the ventral view, they are only separated by 5.5 standard deviations.

These results parallel Reinthal's observation ('90) that MZ and LF can be easily distinguished by vomer rotation but not by vomer width. Rock-dwelling cichlids can be separated into two broad groups based on vomer shape. The first group includes species that have enlarged, horizontally directed vomers, terminal mouths, and feed primarily on plankton either by sucking them from the water column or by brushing them from beds of algae. The second group includes species that have thin, vertically directed vomers, inferior mouths, and feed primarily on attached algae (Reinthal, '90). MZ fits well into the first group. However, LF does not fit well into either group, because it has a ventrally directed vomer like species in the second group and an enlarged vomer like species in the first group.

The width of the vomer at the vomerine notch is independent of width at the palatinad articulation facet. There is no difference in the width of the vomer between MZ and LF where the palatine articulates. Rather, shape difference in the width of the vomer is limited to the vomerine notch, which is associated with the maxilla. Here again, only aspects of shape associated with the oral jaws are different in the skulls of LF and MZ.

There are several general conclusions to be drawn from the results of this morphological study. First, aspects of morphological change between LF and MZ support field observations that these species employ different modes of feeding. Liem ('91) argues that a biting design is merely an "exaggeration" of a suction design. For instance, both designs are characterized by an attenuated cone-shaped buccal cavity and a relatively small mouth gape (Barel, '83). However, biting fish also generally have shorter and more robust jaws. The major trend between LF and MZ is that LF elements are both shorter and more robust. Finally, when examining a structure that is not part of the oral jaw apparatus (e.g., the neurocranium), only those aspects of shape associated with the jaws differ between LF and MZ. This supports the idea that cichlid diversification is expressed mainly in their trophic biology, while the rest of their body remains relatively conserved (Fryer and Iles, '72; Greenwood, '74; Liem, '91).

Geometric approach

The primary objective of this study was to demonstrate the power and utility of geometric morphometrics in describing overall shape change in a complex structure. A major advantage of a

geometric approach is that the analysis is not constrained by focusing on particular shape features a priori. Instead, the method identifies differences in any direction of shape space, providing a more comprehensive and biologically meaningful result.

We do not contend that a geometric approach is best for quantifying specific functional differences between species identified a priori (e.g., the length of a specific moment-arm). Clearly, if this were the goal, direct measures of functionally meaningful characters would be most useful. However, when describing shape change as a whole, it is difficult to relate a series of linear measures to the biology of an organism, especially if any of these measures are correlated. Moreover, many functionally relevant characters have no reliable landmarks.

It was not the goal of this study to quantify these specific differences; rather, on the basis of mode of action, prey choice, and habitat preference in the wild, we assume that MZ and LF differ in terms of feeding performance (McKaye and Marsh, '83; Ribbink et al., '83; Reinthal, '90). Given these differences, we ask what aspects of morphology facilitate these adaptive differences? Once overall shape change is defined, one may wish to formulate and test more specific hypotheses. For example, based on the differences identified above, we would predict that LF has a stronger bite and that MZ is a better suction feeder. These hypotheses could be tested by quantifying the magnitude of difference in biting and suction performance between these two species.

Genetics

LF and MZ could be distinguished from one another in every analysis. Moreover, for every skeletal element, F_1 morphology could be distinguished from both parental species (Fig. 14). This trend suggests an equal contribution of parental alleles to hybrid morphology, and we would predict an additive mode of action for most genes responsible for the morphological differences between LF and MZ. There does, however, seem to be a slight dominance component involving both the premaxilla and the vomer. In both cases F_1 morphology is skewed to-

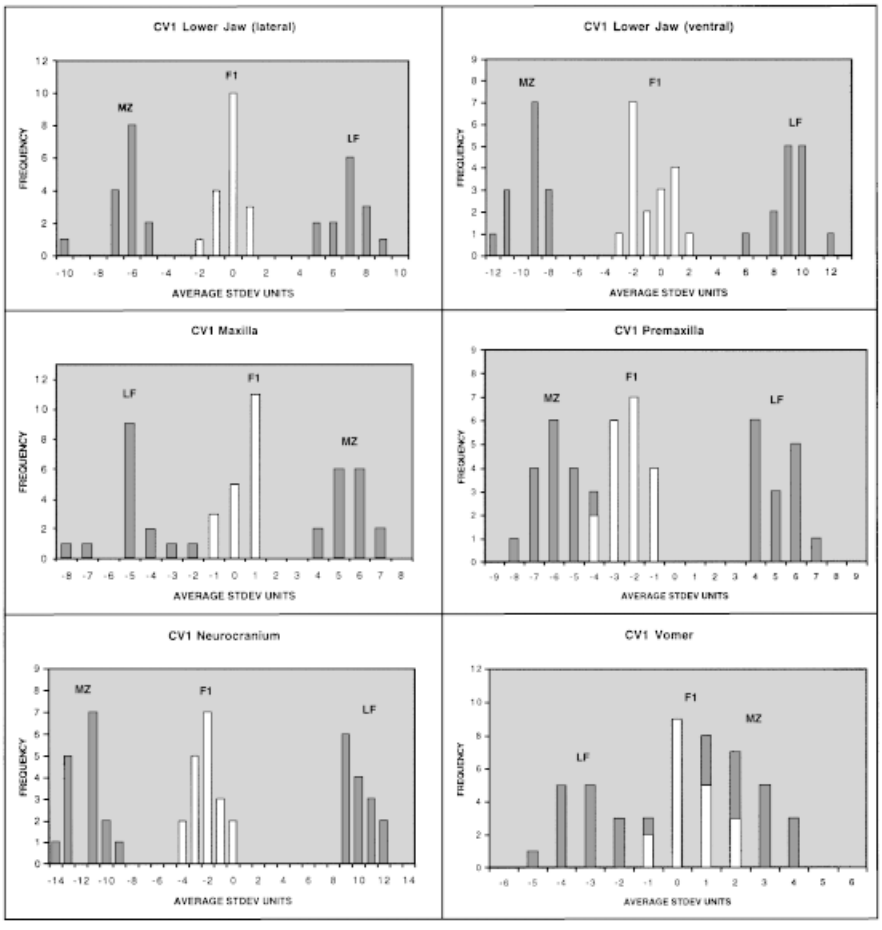

Fig. 14. Histograms showing the position of *M. zebra*, *L. fuelleborni*, and their hybrid progeny along the first canonical variate axis. Since canonical variate loadings are arbitrary units, the *x* axis is recorded in terms of average within-species standard deviation units.

ward that of MZ, and there is considerable overlap in their distributions (Fig. 14). Therefore, certain MZ alleles underlying the premaxilla and vomer may be dominant to LF.

Definitive answers of the genetic architecture and inheritance of these traits are beyond the scope of this study. A thorough examination of F_2 morphology will shed light on the number and mode of action of genes responsible for differences in the oral jaw apparatus. However, detailed knowledge of the genetic architecture of this trait must be based on linking F_2 morphology to molecular markers and genetically mapping these traits in a quantitative trait loci (QTL) analysis. These efforts are already underway.

ACKNOWLEDGMENTS

We thank A. Ambali, the University of Malawi, and the Malawi Government for assistance with collection of specimens and M. Zelditch, K. Liem, J. Bolker, P. Danley, and T. Streelman for technical advice, discussion, and critical reading of the manuscript. Dermestid beetles were provided by M. Scott. All illustrations were done by R. Craig Albertson. This work was supported by the NSF.

LITERATURE CITED

Albertson RC, Markert JA, Danley PD, Kocher TD. 1999. Phylogeny of a rapidly evolving clade: the cichlid fishes of Lake Malawi, East Africa. Proc Natl Acad Sci USA 96:5107–5110.

Barel CD N. 1983. Toward a constructional morphology of cichlid fishes (Teleostei, Perciformes). Neth J Zool 33:357–424.

Barel CDN, Witte F, vanOijen MJP. 1976. The shape of the skeletal elements in the head of a generalized Haplochromis species: *H. elegans* Trewavas 1933 (Pisces, Cichlidae). Neth J Zool 26:163–265.

Bookstein FL. 1989. Principal warps: thin-plate splines and the decomposition of deformations. IEEE Trans Pattern Anal Machine Intelligence 11:567–585.

Bookstein FL. 1991. Morphometric tools for landmark data: geometry and biology. New York: Cambridge University Press.

Crapon de Caprona M-D, Fritzsch B. 1984. Interspecific fertile hybrids of Haplochromine Cichlidae (Teleostei) and their possible importance for speciation. Neth J Zool 34:503–538.

Echelle AA, Kornfield I. 1984. Evolution of fish species flocks. Orono, ME: University of Maine at Orono Press.

Fryer G, Iles TD. 1972. The cichlid fishes of the great lakes of Africa: their biology and evolution. Edinburgh: Oliver and Boyd.

Greenwood PH. 1974. The cichlid fishes of Lake Victoria, East Africa: the biology and evolution of a species flock. Bull Brit Mus Nat Hist (Zool) (Suppl) 6:1–134.

Greenwood PH. 1978. A review of the pharyngeal apophysis and its significance in the classification of African cichlid fishes. Bull Brit Mus Nat Hist (Zool) 33:297–323.

Gower JC. 1975. Generalized Procrustes analysis. Psychometrika 40:33–51.

Kocher TD, Conroy JA, McKaye KR, Stauffer JR, Lockwood SF. 1995. Evolution of ND2 gene in East African cichlids. Mol Phyl Evol 4:420–432.

Lauder GV. 1979. Feeding mechanics in primitive teleosts and in the halecomorph fish *Amia calva*. J Zool (London) 187:543–578.

Liem KF. 1980. Adaptive significance of intra- and interspecific differences in the feeding repertoires of cichlid fishes. Am Zool 20:25–31.

Liem KF. 1991. Functional morphology. In: Keenleyside MHA, editor. Cichlid fishes: behavior, ecology and evolution. London: Chapman and Hall. p 129–150.

Loiselle PV. 1971. Hybridization in cichlids. Buntb Bull 27:9–18.

McElroy DM, Kornfield I. 1993. Novel jaw morphology in hybrids between *Pseudotropheus zebra* and *Labeotropheus fuelleborni* (Teleostei: Cichlidae) from Lake Malawi, Africa. Copeia 1993:933–945.

McKaye KR, Marsh A. 1983. Food switching by two specialized algae-scraping cichlid fishes in Lake Malawi, Africa. Oecologia 56:245–248.

Meyer A. 1993. Phylogenetic relationships and evolutionary processes in East African cichlid fishes. Trends Ecol Evol 8:279–284.

Meyer A, Kocher TD, Basasibwaki P, Wilson AC. 1990. Monophyletic origin of Lake Victoria cichlid fishes suggested by mitochondrial DNA sequences. Nature 347: 550–553.

Moran P, Kornfield I, Reinthal P. 1994. Molecular systematics and radiation of the haplochromine cichlids of Lake Malawi. Copeia 1994:274–288.

Otten E. 1983. The jaw mechanism during growth of a generalized *Haplochromis* species: *H. elegans* Trewavas, 1933 (Pisces, Cichlidae). Neth J Zool 33:55–98.

Owen RB, Crossley R, Johnson TC, Tweddle D, Kornfield I, Davison S, Eccles DH, Engstrom DE. 1990. Major low levels of Lake Malawi and implication for speciation rates in cichlid fishes. Proc R Soc Lond B 240:519–533.

Reinthal PN. 1990. The feeding habits of a group of tropical herbivorous rock-dwelling cichlid fishes from Lake Malawi, Africa. Environ Biol Fishes 27:215–233.

Ribbink AJ, Marsh AC, Ribbink CC, Sharp BJ. 1983. A preliminary survey of the cichlid fishes of rocky habitats in Lake Malawi. S Afr J Zool 18:149–310.

Rohlf FJ. 1999. TPSRegression. Geometric morphometric software for the PC. http://life.bio.sunysb.edu/morph/software.html.

Rohlf FJ, Marcus LF. 1993. A revolution in morphometrics. Trends Ecol Evol 8:129–132.

Rohlf FJ, Slice D. 1990. Extensions of the Procrustes method for the optimal superimposition of landmarks. Syst Zool 39:40–50.

Schulter D, McPhail JD. 1993. Character displacement and replicate adaptive radiation. Trends Ecol Evol 8:197–200.

Seehausen O, van Alphen JJM, Witte F. 1997. Cichlid fish diversity threatened by eutrophication that curbs sexual selection. Science 277:1808–1811.

Stauffer JR Jr, Bowers NJ, Kellogg KA, McKaye KR. 1997. A revision of the blue-black *Pseudotropheus zebra* (Teleostei: Cichlidae) complex from Lake Malawi, Africa, with description of a new genus and ten new species. Proc Acad Nat Sci Philadelphia 148:189–230.

Thompson D'AW. 1917. On growth and form. New York: Cambridge University Press.

Walker J. 1999. Morphometrika. Geometric morphometric software for the Power Macintosh. http://jaw.fmnh.org/Software/Morphometrika.html.

Witte F. 1984. Consistency and functional significance of morphological differences between wildcaught and domestic *Haplochromis squamipinnis*. Neth J Zool 34:596–612.

Yaroch LA. 1996. Shape analysis using the thin-plate spline: Neanderthal cranial shape as an example. Yearb Phys Anthropol 39:43–89.